UPTEC X 03 014
MAY 2003

ISSN 1401-2138

ANDERS BJURSTRÖM

Functional studies of VCP

Master’s degree project

UPPSALA UNIVERSITET

Molecular Biotechnology Programme

Uppsala University School of Engineering

UPTEC X 03 014	**Date of issue 2003-05-22**

Author

Anders Bjurström

Title (English)

Functional studies of VCP

Title (Swedish)

Abstract

A kinetic assay was developed and used to characterize the ATPase activity of VCP and to find and measure the effect of interacting biological components. One such component, p47, was analyzed with circular dichroism in order to retrieve structural information. Together with kinetic results, measurements with isothermal titration calorimetry and light scattering gave interesting information of the role of different domains of VCP. The structure of AAA ATPases in general and of VCP is reviewed, and an interesting structural motif was submitted to a database in search for structural homologs.

Keywords

VCP, AAA ATPase, p47, kinetics, mutants

Supervisors

Axel T. Brünger
Stanford University

Scientific reviewer

T. Alwyn Jones
Uppsala University

Project name	Sponsors **Howard Hughes Medical Institute**
Language **English**	Security
ISSN 1401-2138	Classification
Supplementary bibliographical information	Pages **23**

Biology Education Centre Biomedical Center Husargatan 3 Uppsala
Box 592 S-75124 Uppsala Tel +46 (0)18 4710000 Fax +46 (0)18 555217

Functional studies of VCP

Anders Bjurström

Sammanfattning

VCP (valosin containing protein) är namnet på ett protein som man fortfarande inte riktigt vet hur det fungerar eller exakt vad det gör. Olika experiment visar att det verkar ha funktionen att ta bort andra proteiner som inte fungerar som de ska, och även att sammanfoga membran i den s k golgiapparaten, som fragmenteras när cellen delar sig. För att kunna utföra dessa uppgifter använder VCP kemisk energi som finns i den biologiska molekylen ATP. För att hitta de komponeter i cellen som är viktiga för VCP's funktion kan man mäta hur fort ATP-molekylerna förbrukas. Om en viss komponent gör att ATP förbrukas fort av VCP, har den troligen en roll i dess funktion. Förutom dessa mätningar undersöks det i detta arbete vad som händer med proteinet när man byter ut vissa specifika aminosyror, som är byggstenarna i alla proteiner. Tillsammans kan resultaten från dessa experiment ge information om VCP's uppgift i cellen, samt vilken roll de olika delarna av proteinet har i dess funktion.

Examensarbete 20p i Molekylär bioteknikprogrammet

Uppsala Universitet Maj 2003

Table of contents

1. Introduction

1.2 VCP

VCP (Valosin Containing Protein) is a large hexameric protein (540 kDa) that is abundant in all cell tissues and essential for viability in a wide range of organisms. Based on its primary sequence, VCP is a member of the AAA family of ATPases (ATPases associated with various cellular activities), which includes a wide range of mechanoenzymes that act on their substrate upon hydrolysis of ATP. This work is mainly focused on the ATPase kinetics of VCP from mouse (*Mus musculus)*. Combined with structural studies, the objective is explore the functionality of the enzyme by characterizing the ATPase kinetics of the wildtype, compare with different conditions and mutants, and see how the activity is affected by possible binding partners.

Much research has been done to elucidate the function of VCP, but it is not yet fully understood. It is well established that VCP is important in various membrane fusion events, perhaps similar to its relative NSF (N-ethylimide Sensitive Factor), an AAA ATPase that recycles SNARE proteins involved in pre-synaptic vesicle fusion (1). p47 is a protein that is found in complex with VCP, and both proteins are required for fusion of post-mitotic golgi fragments (2). VCP has a yeast homologue called Cdc48 after the discovery that mutations in of this protein results in arrest in the cell division cycle. Cdc48 has also been implicated in fusion of ER and of outer nuclear envelopes in yeast karyogamy (3).

A different role that has been proposed for VCP is in the ubiquitin dependent degradation pathway. Cdc48 binds Ufd1-3 and Npl4, which are involved in the degradation of ubiquitin fusion proteins, and it is needed for the export of ubiquitylated proteins from the ER (4). Misfolded soluble and membrane associated test proteins showed significantly increased stability in both Cdc48 mutants and Npl4/Ufd1 mutants. Similar results were obtained with mammalian VCP. It is also shown in (4) that p47 inhibits the release of poly-ubiquitylated MHC heavy chains into the cytosol. This result goes in line with the finding that p47 and the Ufd1-Npl4 (UN) complex bind to VCP mutually exclusively (5). The two binding partners have been proposed to act as adaptors of VCP, recruiting the enzyme for different tasks. The UN complex does not seem to have a role in golgi fusion (5), but interestingly, VCP-p47 can bind mono-ubiquitylated protein conjugates, and the ability of p47 to bind ubiquitin was shown to be required for the fusion of golgi fragments (6). VCP-UN on the other hand, has a high affinity for proteins that have been poly-ubiquitylated, a signal that is used in ubiquitin dependent degradation. It can also bind to mono-ubiquitylated conjugates, but less efficiently than the VCP-p47 complex. The UN-complex exists independently, but p47 is only found in complex with VCP (6).

1.2 AAA ATPases (7, 8, 9, 10)

AAA ATPases belong to a larger family of proteins, the P-loop NTPases which all contain motifs called Walker A and B in their nucleotide-binding domain. These motifs consist of conserved residues forming a structured loop (the P-loop) and parts of helices in the nucleotide-binding pocket. The Walker A contains an important lysine residue that is involved in nucleotide binding, and the Walker B contains a glutamate residue that coordinates a magnesium ion - an important activating ion in nucleotide hydrolysis. AAA ATPases typically have an N-terminal domain, which has been proposed to interact with substrate, and one or two nucleotide-binding domains (D1 and D2). The nucleotide-binding domain has an N-terminal subdomain, where the nucleotide binds, and a C-terminal helical subdomain (figure 1.1). This architecture characterizes the AAA+ superfamily.

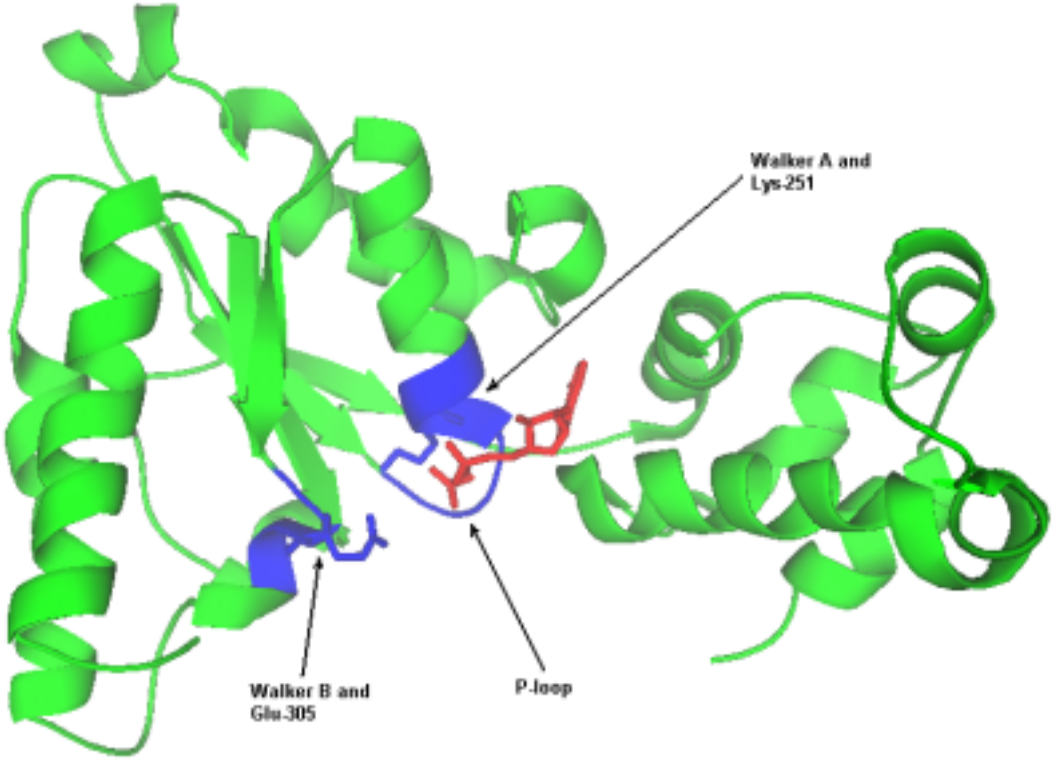

Figure 1.1: D1-domain of VCP with bound ADP. The left part is the N-terminal subdomain, and on the right is the C-terminal helical subdomain.

The N-terminal subdomain of the nucleotide-binding domain has a αβα-fold with a central β-sheet made up of 5 parallel strands of order 51432. The insertion of β4 separates the Rec-A like NTPases from other P-loop NTPases. A polar residue at the end of β4, between the P-loop and a conserved aspartate in the Walker B motif, has been named sensor-1 because it makes contact with the γ-phosphate of the nucleotide, and would be able to distinguish between ADP and ATP. In VCP-D1, the sensor-1 is Asn-348.

The C-terminal part of the nucleotide-binding domain is mostly helical. A recurring feature of this subdomain is a residue (typically arginine) called sensor-2 for its ability to interact with the nucleotide. A study of Hsp104 has indicated that its primary role is to provide binding energy rather than distinguish ADP from ATP (11).

AAA proteins have the ability to oligomerize into ring conformations, typically as hexamers, with the nucleotide bound at the subunit interface. A conserved arginine residue in the N-terminal end of β5 has been named the 'arginine finger' and is important for inter-protomer communication and cooperativity in ATP hydrolysis. All AAA+ proteins share this feature. In AAA proteins, the arginine finger is connected to the sensor-1 by a series of highly conserved residues containing a α-helix. This has been called the second region of homology (SRH) and defines the AAA class of ATPases. In VCP, the arginine finger is Arg-359.

In many cases, oligomerization of the ATPase is nucleotide dependent. The enzyme katanin for example, which acts on microtubules, only oligomerizes transiently on its substrate upon ATP binding (12). In the case of ATPases with two nucleotide-binding domains, the hexameric state is more stable. NSF only disassembles on nucleotide release and VCP exists exclusively as a hexamer. In these two examples, only one of the nucleotide-binding domains is responsible for the major part of the ATPase activity (13 and this study). Since the ATP-bound state promotes oligomerization in the katanin case, a duplication and subsequent loss of hydrolytic activity may have been selected for in evolution as a means of maintaining the enzyme in its active hexameric state.

1.3 Structure of VCP

VCP is a hexameric complex of 89.5 kDa subunits. Each subunit consists of an N-domain and two nucleotide-binding domains, D1 and D2. During the ATP cycle, VCP undergoes conformational changes. The main events during the ATP cycle are ATP binding, ATP hydrolysis, phosphate release and ADP release. The shape of VCP in four nucleotide states has been studied with electron microscopy (14). The nucleotide states are ADP, ATP-analog, transition state-analog (ADP-AlF_x), and ADP-P_i analog. Significant movements could be seen in the nucleotide-binding domains. The N-domain was only visible in the ADP-AlF_x state, indicating that it is flexible. Until recently, the only high-resolution structure of VCP was from the truncated N-D1 domain, but a 4.7 Å crystal structure of the full length protein has now been completed in a mixed ADP/ADP-AlF_x state by Byron Delabarre at Stanford University (submitted for publication). As opposed to the N-D1 structure, which was a crystallographic hexamer, the full-length diffraction data was processed with a two-fold rotation axis coincident with the molecular six-fold, having three protomers in the asymmetric unit. Although the three protomers did not show any large differences in the crystal structure, it might be that they do not all have the same conformation simultaneously in vivo. Initial phases were obtained using the N-D1 structure for molecular replacement. Further improvements were accomplished using Se-Met MAD phasing and B-factor sharpened amplitudes. The D1 and D2 domains are positioned head to tail on top of each other, and as anticipated by the high level of

similarity (66%), the structures of the two domains are very similar. The diameter of the hexamer is 143 Å at the D2-domain and 156 Å at the D1, where the N-domain is situated radially. There is a waist between the D1- and D2-domain of 90 Å, and the overall height is 85 Å. There is a central pore along the symmetry axis about 20 Å wide but seems to be completely blocked at a point in the D1-domain where six histidines point in towards a ligated zinc atom. As no salts containing zinc had been added to the growth medium or any of the purification buffers, it must be of bacterial origin. A more detailed description of tertiary structure of VCP above the general features from the AAA ATPase section will not be relevant in this work.

2. Methods

2.1 Transformation, Growth and Purification

VCP and mutants thereof were expressed in the *E Coli* strain BL21-DE3-RIL using a pET-28a construct. This plasmid has kanamycin resistance and N-terminal thrombin cleavable his_6-tag. It carries the T7 promoter, which is controlled by the lac operon. BL21 is the most widely used host and has the advantage of being deficient in both lon-1 and ompT proteases. The designation DE3 indicates that the strain is a lysogen of lDE3, and therefore carries a chromosomal copy of the T7 RNA polymerase gene under control of the lacUV5 promoter. RIL indicates that the cells have the tRNA anti-codons needed for expression of eukaryotic genes. Induction is started by the addition of the galactose analogue IPTG (Isopropyl-1-tio-beta-D-galactoside), which inhibits the repressor of the T7 promoter. Novagen Rosetta cells, which have another three eukaryotic codons, were also used for expression of the VCP mutant K524A. For transformation and growth of the Rosetta cells, both chloramphenicol and kanamycin was used.

Harvested cells were incubated with buffer containing lysozyme, BME and EDTA-free Complete anti proteolysis tablets, and then lysed by sonication. The initial purification step was his_6-tag binding to Ni-NTA resin and subsequent elution with an imidazole gradient. The his_6-tag was cut with thrombin for VCP and TEV for p47. Subsequent purification steps were ion exchange chromatography (mono-Q) and gel filtration (Superdex S75 for p47 and S200 for VCP). All purification steps were done at 4ºC.

For minipreps of mutant DNA, DH5-α cells were used. These cells have high plasmid copy number and also have important DNAses removed.

The mutants that were used in this work were the D1 nucleotide-binding mutant K251A, the D2 nucleotide-binding mutant K524A and the D2 hydrolysis mutant E578Q (although never successfully purified). The lysine involved in nucleotide binding makes favorable electrostatic interactions with the β-phosphate of the nucleotide and the glutamate coordinates the Mg^{2+} ion needed for ATP hydrolysis.

2.2 Coupled ATPase assay

The rate of ATP hydrolysis was measured continuously using a Spectramax plate reader (Molecular Devices). Up to 96 reaction wells can be followed spectrometrically during the reaction at one or more wavelengths. The release of inorganic phosphate is detected by a secondary reaction in which purine nucleotide phosphorylase (PNP) converts 2-amino-6-mercapto-7-methylpurine riboside (MESG) to ribose 1-phosphate and 2-amino-6-mercapto-7-methylpurine. This reaction shifts the absorption maximum from 330 nm to 360 nm and allows for spectrometric quantification (figure 2.1) (15).

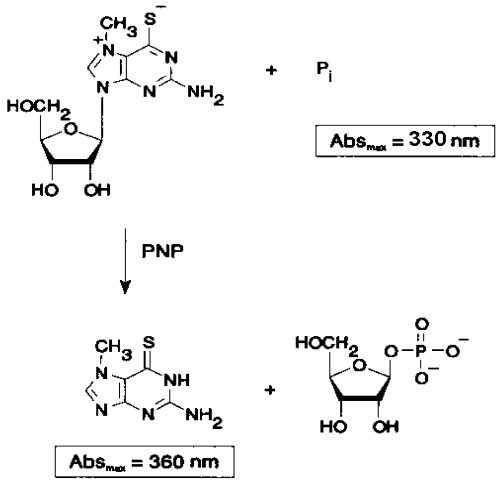

Figure 2.1: In the presence of inorganic phosphate, PNP converts MESG to a product that has peak absorbance at a different wavelength.

A phosphate assay kit from Molecular Probes was used. The working mix contains 50 mM Tris-HCl pH 7.5, 8 mM $MgCl_2$, 0.1 mM NaN_3, 200 μM MESG and 1 unit PNP/ml (one unit PNP converts 1 μmole MESG to product per minute at 25ºC and pH 7.4). The reaction mix contained working mix, 0.5 μM $VCP_{protomer}$, and indicated concentrations of ATP or ADP. Both substrate and enzyme solution was first preincubated with working mix to consume possible phosphate contaminations. The reaction was then started by adding the enzyme solution to the substrate solution, making up a reaction volume of 250 μl. The experiments were done at 37°C. Using an ATP:$VCP_{protomer}$ molar ratio of 2000, the maximum turnover rate is approximated by the initial slope of the plot of the phosphate response vs. time. The statistics in the plots is based on four independent measurements.

2.3 Light scattering (16)

The degradation fragments that emanated from the purification of the K251A mutant were investigated by light scattering, which is a well-established method for investigating molecular weight, size, shape and solvent interactions of various biological and non-biological polymers. Monochromatic light is sent through the sample and scattered light

is measured at different angles. Macromolecules will scatter incoming light depending on concentration, refractive index, size and polarizability. The following equation describes the scattering in the experiment:

$$\frac{Kc}{R(\theta)} = \frac{1}{M_W P(\theta)} + 2A_2 c$$

where

$$K = \frac{4\pi^2 \left(\frac{dn}{dc}\right)^2 n_{solv.}^2}{N_A \lambda^4}$$

n is the refractive index of the sample and c is the concentration of the sample. N_A is the Avogadro constant and λ is the wavelength of the light (690 nm in these experiments). R(θ) is the scattered light in a certain angle in excess of the light scattered by the solvent, normalized to the distance to the sample, the volume of the illuminated sample, and the intensity of the incident ray. M_w is the weight average molecular weight (see below), and P(θ) is the scattering function: The variation of scattered light with angle is determined by the mean square radius of the molecule. A bigger radius results in greater angular variation. A_2 is the second virial coefficient, describing solvent/solute interactions.

Weight average molecular weight $$M_W = \frac{\sum_i n_i M_i^2}{\sum_i n_i M_i}$$

Number average molecular weight $$M_N = \frac{\sum_i n_i M_i}{\sum n_i}$$

If the ratio of weight average and number average molecular weight is close to one, the sample is said to be mono-disperse, which is an indication of good sample quality.

In this work, light scattering is coupled to size exclusion chromatography (HPLC-SEC) with the objective of finding the molecular weight. Having calibrated the system with BSA, the sample concentration at the different time points is known. At low concentrations,

$$\frac{Kc}{R(\theta)} = \frac{1}{M_W}\left[1 + \frac{16\pi^2}{3\lambda^2} < r_g^2 > \sin^2(\theta/2)\right]$$

where $<r_g^2>$ is the mean square radius of gyration. Plotting $Kc/R(\theta)$ against $\sin^2(\theta/2)$ at each time point gives $Kc/R(\theta)$ intercepts at $1/M_w$.

2.4 Circular Dichroism (17, 18)

p47 was examined for structural changes in the presence of phosphatidyl ethanolamine with circular Dichroism, which is a method that can be used to get information about the secondary structure contents of proteins. The property that this technique is based upon is the optical activity of the asymmetric α-carbons in the peptide chain. Depending on secondary structure and wavelength of an incident ray of light, left and right handed circularly polarized light will be affected differently and give rise to a signal that can be decomposed into contributions from different structural elements.

Linearly polarized light can be viewed as a superposition of two rays of the same amplitude and phase, circularly polarized in opposite directions (figure 2.3A). As this light passes through a material that has different absorbance for the different directions of circular polarization, the resulting superposition will no longer be linear but elliptical. The occurrence of ellipticity is called circular dichroism, but it does not itself change the angle of polarization. The angle of polarization is changed when the refracting index of a material is different for left and right handed polarized light (optical birefringence). This change in polarity (optical rotation) is caused by a phase shift between the two components (figure 2.3B).

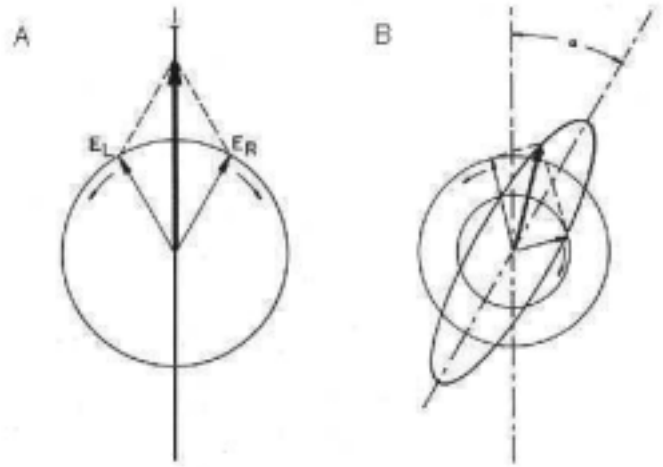

Figure 2.3A: Linearly polarized light as a superposition of two rays that are circularly polarized in different directions. B: If absorbance and refractive index of a material is different for the two rays, it will cause ellipticity and optical rotation.

Actually, circular dichroism does not exist without optical rotation, and they are related by a Kronig-Kramers transformation (19). The relative difference in absorbance is very small, usually between 0.0001 and 0.001, and the optical rotation is in the millidegree range.

The optical rotation is plotted against wavelengths between 180 and 260 nm. For a quantitative analysis of secondary structures, the wavelength scan can be decomposed using singular value decomposition (SVD) and reconstructed using only the most significant eigenvalues and their respective eigenvectors. Wavelength scans beyond 180

nm give enough information to use four basis spectra and accurately reproduce the plot. Truncated wavelength scans give less accurate results, but the α-helical contribution can always be confidently predicted, since this is the dominant signal in the spectrum. Figure 2.4 shows the contributions from different secondary structure elements.

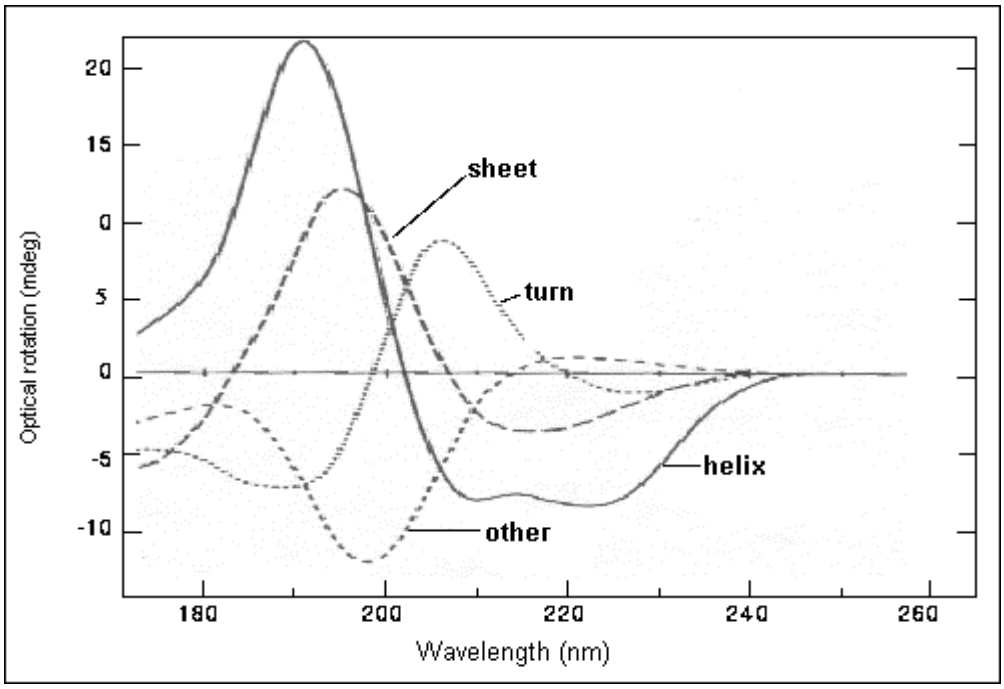

Figure 2.4: Circular Dichroism of different secondary structures.

2.5 Isothermal titration calorimetry (20, 21)

The energetics of ADP binding to VCP was investigated with ITC. This is an established technique for investigating both protein-protein interactions and macromolecular interactions with smaller molecules. The instrumentation is composed of a sample cell and a reference cell enclosed in an adiabatic jacket. The reference cell generally contains buffer or water. As ligand is injected in the sample cell containing the macromolecule solution, heat is either absorbed or produced. Detectors sense the difference in temperature between the sample cell and the reference cell, and the electrical power it takes to keep the temperature constant is recorded and plotted. Each injection give rise to a peak, the area of which corresponds to the heat change coupled to the binding event. As the binding sites become saturated, the peaks get smaller and smaller until the only the heat produced is that of dilution and non-specific interactions. Along with the differential power signal, the heat change for each injection, Δq_i is normalized to the amount of added ligand, $\Delta[L]_i$, and plotted against the total ligand concentration $[L_T]$. Ideally this produces a sigmoid curve, and it corresponds to $dq/d[L_T]$ as a function of $[L_T]$. The binding stochiometry, n, the enthalpy of binding, ΔH, and the association constant, K_A, can be determined by a non-linear regression procedure after fitting the following equation to the data:

$$\frac{dq}{dL_t} = \Delta H\left(\frac{1}{2} + \frac{1 - X_R - r}{2\sqrt{(1 - X_R - r)^2 - 4X_R}}\right)$$

where $X_R=[L_T]/[M_T]$ and $r = 1/K_A[M_T]$.

This equation is called the Wiseman equation and the derivation can be found in (22).

2.6 Mass Spectrometry

Electrospray-TOF and Maldi-TOF was used to determine molecular weights of VCP fragments and p47. Molecular weight calculation of a given number of residues from the sequence was done using the PeptideMass tool at the Expasy server (www.expasy.org/tools).

3. Results

3.1 Growth and purification of p47 and VCP mutants

p47 purifies nicely using Ni-chromatography, ion-exchange chromatography and gel filtration. SDS-PAGE gels from the two latter purification steps are shown in figure 3.1. Successful TEV-cutting of the his_6-tag was confirmed by mass spectrometry (p47 weighs 40.9 kDa).

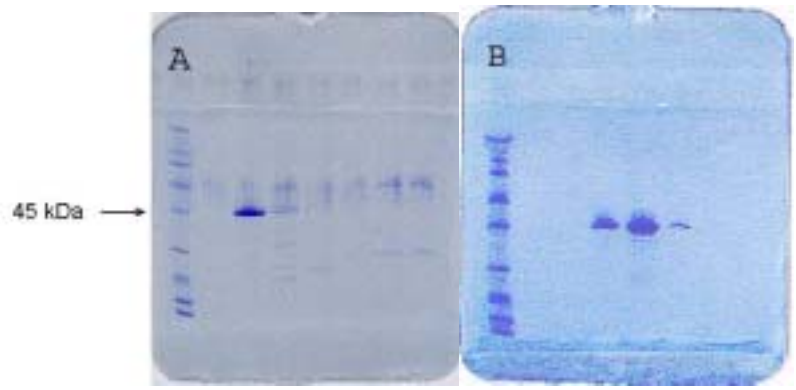

Figure 3.1: Purification of p47. A: SDS-PAGE gel of the Mono-Q fractions. B: SDS-PAGE gel of the gel filtration fractions.

The VCP mutants were more difficult to purify. Induction of VCP works well (K524A induction shown in figure 3.2A), but all three mutants showed extensive degradation after Ni binding and elution with imidazole. The fractions of the K524A mutant from the Ni elution contained some non-degraded protein (figure 3.2B), and enough material was eventually recovered to do some initial experiments. The bands of the Mono-Q fractions

were barely visible but after concentrating, the gel shows bands at the right molecular weight that were estimated to be 90% pure (figure 3.2C).

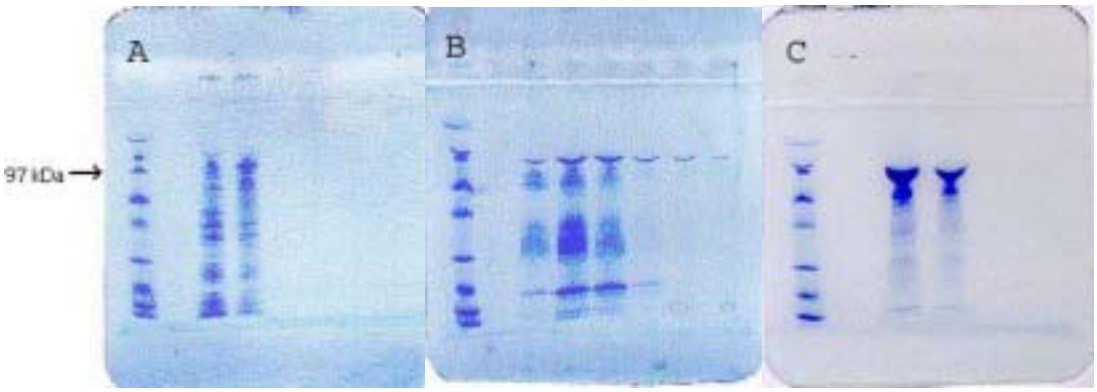

Figure 3.2: SDS-PAGE gels from the purification of VCP K524A. A: Samples before and after induction. B: Fractions from the Ni-column. C: Concentrated sample after Mono-Q (two dilutions).

The fractions of a nice baseline-separated absorption peak from the nickel column-elution of K251A showed two bands close to the 65-kDa marker on the gel (figure 3.3A). The slightly different degradation products separate on a mono-Q column (figure 3.3B) and are referred to as sample 1 and 2, respectively. Sample 2 was run on a native gel together with wildtype VCP. Wildtype VCP remains in its hexameric state in a variety of conditions such as high salt and high temperature (Byron Delabarre, personal communication). Even the truncated N-D1 form of the protein is a stable hexamer. It is therefore interesting that the K251A mutant comes out as something else, which is evident from the gel in figure 3.3B.

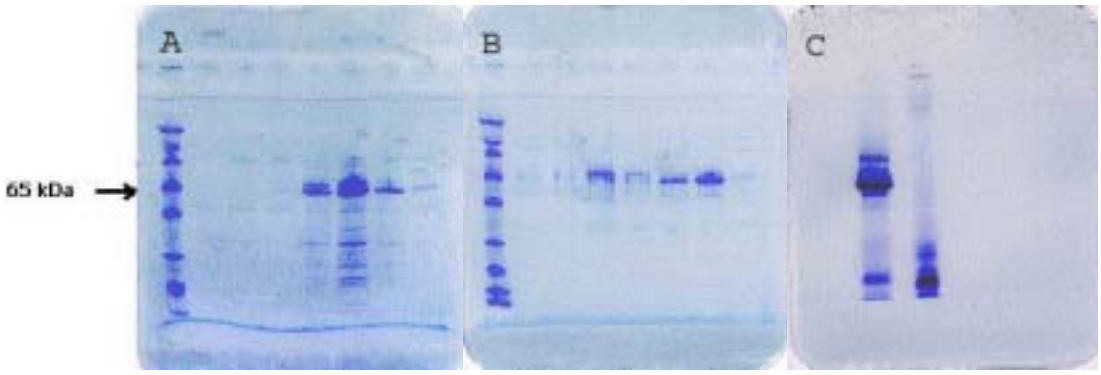

Figure 3.3: Purification of VCP-K251A. A: SDS-PAGE of the fractions from the Ni column. B: SDS-PAGE of the fractions from the Mono-Q column. C: Native PAGE gel of wildtype VCP and K251A respectively.

To find the oligomeric state of VCP-K251A, the samples were run on a gel filtration column connected to light scattering equipment. Figure 3.4 shows the scattering plots from sample 1. The weight of the molecules that give rise to the first peak corresponds to a hexamer, and the second peak has an apparent weight of 104 kDa, which would be the approximate weight of a truncated dimer.

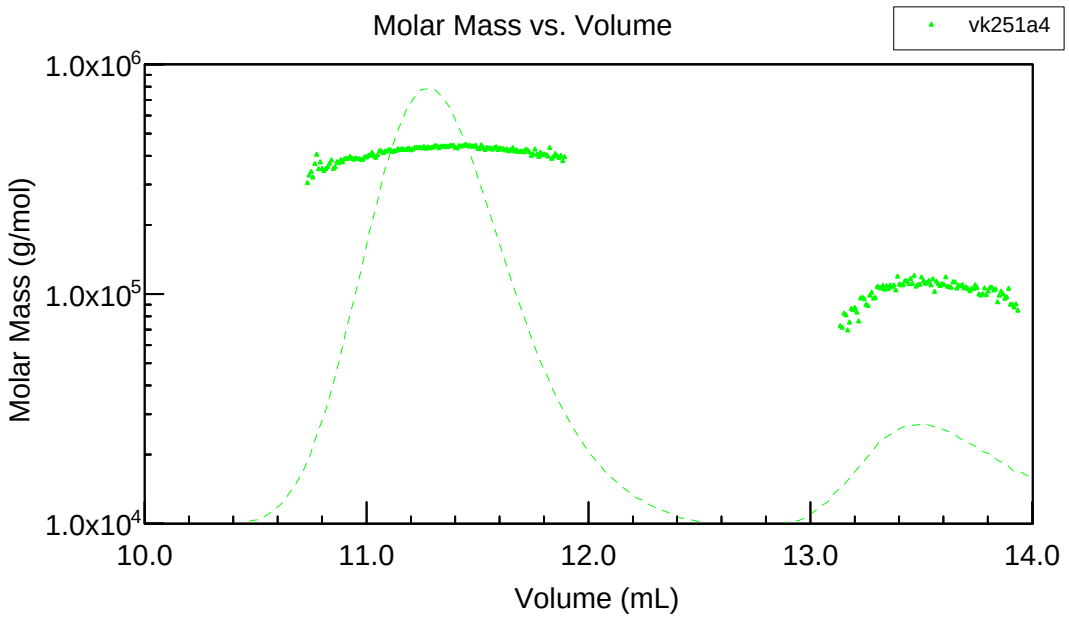

Figure 3.4: Light scattering result from VCP K251A. The peaks are 90 degree light scatter and the dots correspond to the weight average molecular weight, which has been calculated from the light scattering.

The light scattering of sample 2 showed that it was pure dimer, in accordance with the gel in figure. 3.3C.

The sample was also analyzed with mass spectrometry in order to get a molecular weight of higher accuracy. Electrospray-TOF did not work for some reason, but MALDI-TOF gave a molecular weight of 66.5 ± 0.8 kDa per protomer. It is assumed that the N-terminal is intact since the protein was bound to the nickel column. 66.5 kDa corresponds to the N-terminal 601 residues out of the full length number of 806, but taking the error of measurement into account, the cleavage site could be at any residue from 593 to 608. Residue 601 and neighboring residues are normally situated in the central pore, but are exposed if the protein fails to form hexamers. Residues 598-600 are in a loop, so the cleavage point is likely to be at one of those residues. The K251A truncated dimer had no ATPase activity.

3.2 Circular dichroism of p47 + PE

The proposed adaptor protein of VCP, p47, seems to be poorly structured on its own. It does not crystallize, and CD-melts does not show any transition point in the 222 nm signal (where α-helices have their strongest signal) (Byron Delabarre, personal communication). However, studies using FTIR-spectroscopy have indicated that some structural events take place when phosphatidyl ethanolamine (PE) is added to p47 (23). To further investigate this, CD-melts of p47 were done in the presence of PE with either 6 or 8 carbons in the acyl chain. Approximately 3 and 10 molar excess of PE was used respectively, and the melts were done at pH 5.7 and 8.0. The CD-signal at 222 nm was

recorded for possible transition points when α-helices denatures. No such features emerged though. All the melts looked more or less like the one in figure 3.5B, and further structural analysis of p47 was abandoned.

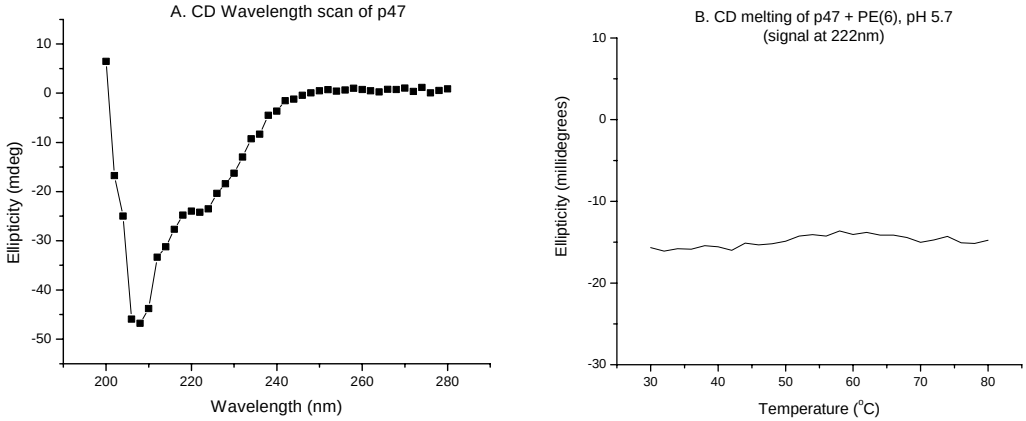

Figure 3.5: Circular dichroism of p47. A: Wavelength scan of p47 alone. B: Absorbance at 222 nm (α-helix peak signal) during melting of p47 + PE.

3.3 Apyrase kinetic assay

To validate the method used for measuring ATPase kinetics, initial measurements were made on apyrase, an enzyme that can hydrolyze both ATP and ADP at documented rates. This enzyme exists in two different forms. The A-form hydrolyzes ATP ten times as fast as ADP. The B-form hydrolyzes ATP and ADP at the same rate. To limit the reaction to only one hydrolysis event per nucleotide, ADP was used as substrate, and the B-form of apyrase was chosen because it is more active with ADP as substrate. Using the software provided with the plate reader, the initial slopes at different concentrations of ADP were measured (figure 3.6)

From a phosphate standard curve it was calculated that 1 $mUnit_{abs}$ corresponds to 0.143 μM P_i. The rates from the plate reader software are given in mU_{abs}/min and the conversion to μmol*min^{-1}*mg_{enz}^{-1} (μkat) is done in the following way:

$$\frac{mU_{abs}}{\min} * \underbrace{\frac{\mu M}{mU_{abs}} * L * \frac{1}{mg_{enz}}}_{conversion-factor} = \mu mol * \min^{-1} * mg_{enz}^{-1}$$

The plot of the results is shown in figure 3.7A. The kinetic parameters k_{cat} and K_M were calculated using an Eadie-Hofstee plot as shown in figure 3.7B. They are listed together with earlier published results in table 3.1.

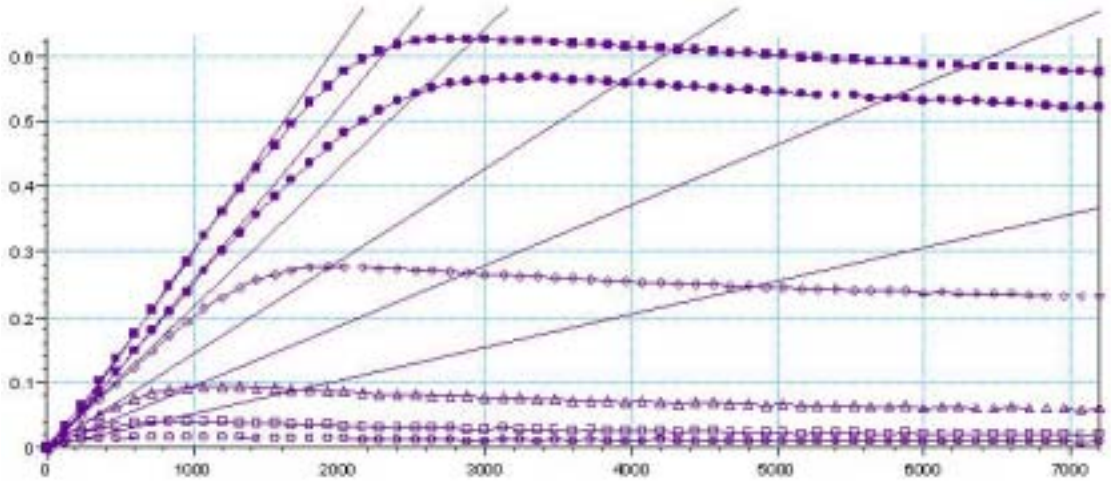

Figure 3.6: ADPase assay with different concentrations of ADP. Dotted lines: absorbance units versus time (sec). Straight lines: Initial (maximum) rate of phosphate release.

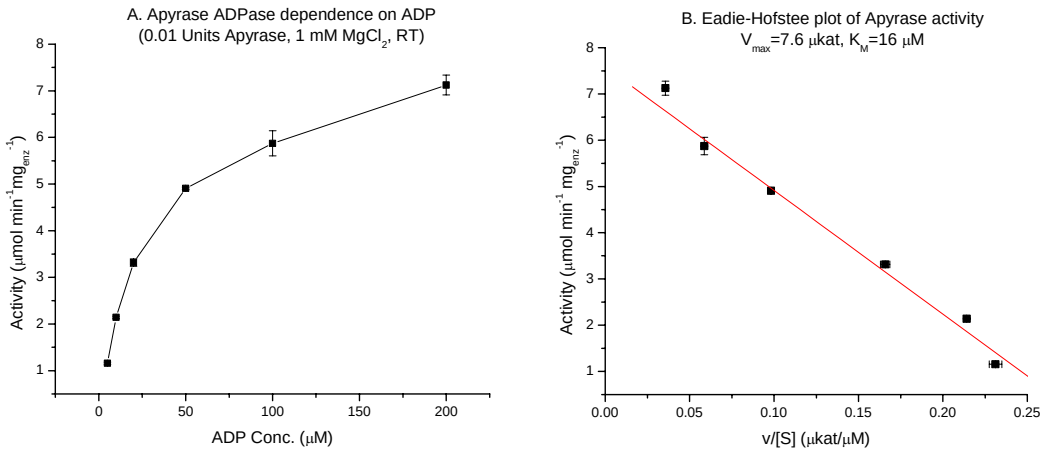

Figure 3.7A: Initial turnover rates of apyrase at different ADP concentrations. B: Eadie-Hofstee plot of the data points in A.

Table 3.1 Comparison of different results of V_{max} and K_M of apyrase.

	V_{max}	K_M
Bjurstrom, 2002	7.6 µkat	$1.6*10^{-5}$ M
Molnar, Lorand, 1961	82 µkat	$2.4*10^{-5}$ M
Kettlun et al., 1982	9.2 µkat	$0.7*10^{-5}$ M

The purpose of the apyrase validation was to make sure that the assay gives reasonable results in the same range as earlier experiments. The exact numbers will depend on protein preparation, reaction buffer components, temperature and the method used for measuring the release of phosphate. The results from the apyrase assay show that the continuous flow method is working and allows for measurements of kinetic constants.

3.4 VCP kinetic assays

Mg^{2+} has been shown to be an activating ion in ATP hydrolysis. To optimize conditions for the activity of VCP, an assay was carried out with constant ATP concentration (1 mM) and various concentrations of $MgCl_2$. The highest activity was obtained at 8 mM $MgCl_2$ as shown in figure 3.8A. To check if this is a general property of divalent metal ions or specific for magnesium, similar experiments was done with $CaCl_2$ and $ZnCl_2$. Zn^{2+} seemed to interfere with the assay, which also was confirmed by making a standard curve of phosphate with $ZnCl_2$ present. The plot with $CaCl_2$ is shown in figure 3.8B. $CaCl_2$ has only a deactivating effect on VCP, which suggests that VCP is activated by Mg^{2+} specifically.

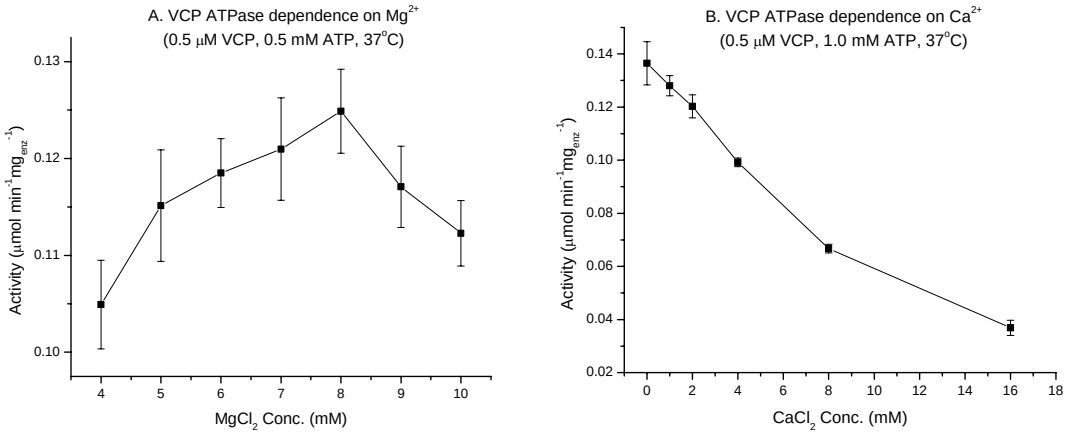

Figure 3.8: ATPase activity dependence on $MgCl_2$ (A) and $CaCl_2$ (B).

Initial studies on how the ATP hydrolysis rate is dependent on the concentration of ATP were the made in the range of 0.2-5.0 mM ATP. To show the effect of Mg^{2+}, the experiment was done with 1 mM and 8 mM $MgCl_2$ respectively. The results can be seen in figure 3.9.

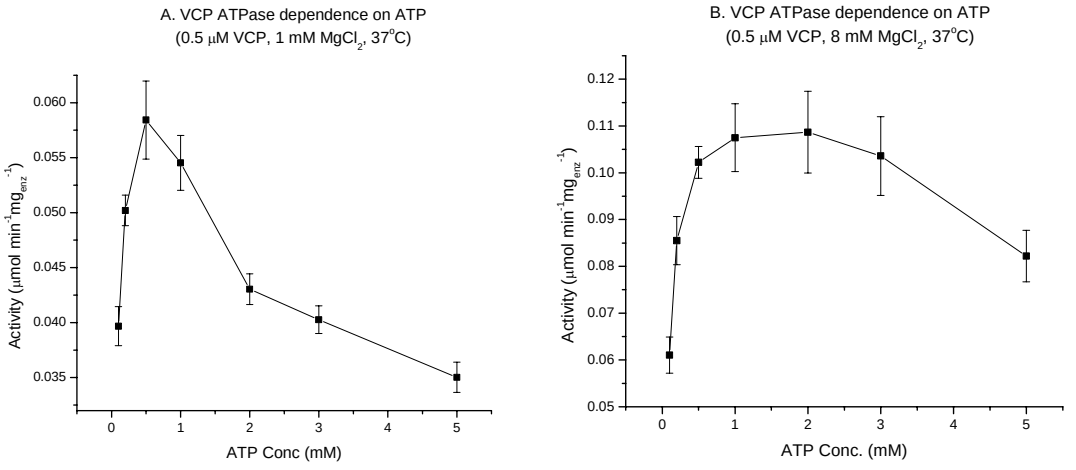

Figure 3.9: ATPase Activity of VCP at different ATP concentrations. The reaction mix in A contains 1 mM $MgCl_2$, and the reaction mix in B contains 8 mM $MgCl_2$.

The most apparent and surprising feature of the plots in figure 3.9 is that the activity decreases at higher ATP concentrations. A suggestion that was made was that more ADP is produced in a pre-steady state phase at higher ATP concentrations and acts as a competitive inhibitor. The measurement technique does not detect the phosphate that is released in that early process since the first measurement is set as the zero point. To investigate the possibility of ADP inhibition, enzymatic assays with different concentrations of added ADP were done. The result is shown in figure 3.10A, and indeed VCP seems to have a much higher binding affinity for ADP since the activity is effectively decreased even at low ADP-ATP ratio. Lineweaver-Burke plots with different amounts of ADP confirmed competitive inhibition and Michaelis-Menten like behavior, although linearity is not quite within the range of error (figure 3.10B).

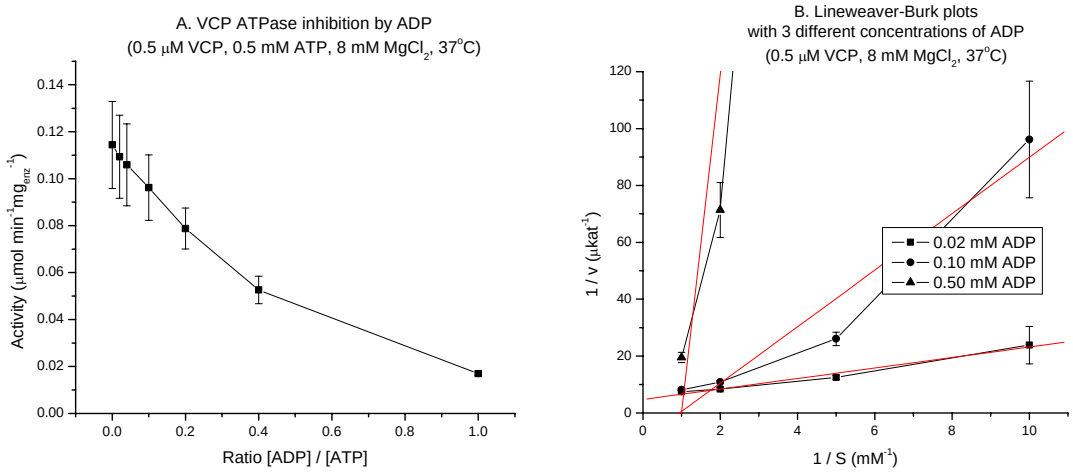

Figure 3.10: ADP Inhibition. A: Rate of ATP hydrolysis with different amounts of ADP. B: Lineweaver-Burke plots with different amounts of ADP. The results indicate competitive inhibition.

To obtain values of V_{max} and K_M, a set of assays were done in the 0.1-1.0 mM ATP range, where the ADP inhibition has not yet become significant. The results are shown in figure 3.11 along with an Eadie-Hofstee plot. From the Eadie-Hofstee plot, V_{max} was estimated to 0.14 μkat, and K_M to 0.13 mM (table 3.2).

Table 3.2: Kinetic constants of VCP estimated from an Eadie-Hofstee plot.

V_{max}	**0.14 μkat**
K_M	**0.13 mM**

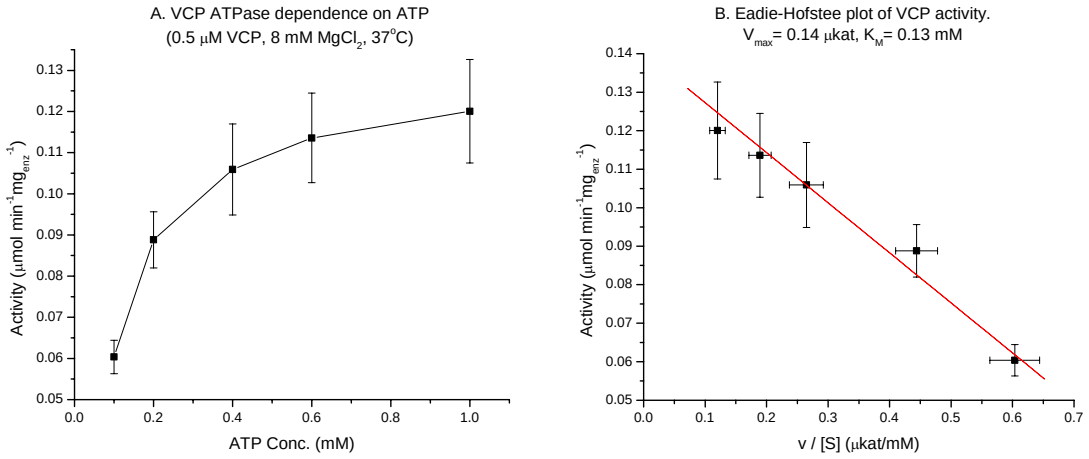

Figure 3.11A: Initial turnover rates of VCP at different ATP concentrations. B: Eadie-Hofstee plot of the data points in A.

3.5 Effect of p47 and ubiquitin

As discussed earlier, p47 is a known binding partner of VCP. Published data shows p47 to have an inhibitory effect on the ATP hydrolysis of VCP (24). Since VCP has also been implicated in the ubiquitin dependent degradation pathway, it would be interesting to see if ubiquitin has an effect on the activity of VCP. The Ufd1-Npl4 complex is thought to be needed in this pathway, but p47 has in fact also a binding affinity for ubiquitin. In the first experiment, VCP was incubated with p47 in different amounts before it was mixed with a solution containing 1 mM ATP. At a low p47-VCP molar ratio the activity significantly decreases, but increases slightly again as the amount of p47 gets higher (figure 3.12). The same experiment was then done in the presence of 1 and 4 molar equivalences of ubiquitin to the VCP hexamer, respectively. The results from these measurements were identical to the one without ubiquitin, so the conditions needed for interaction between VCP and ubiquitin do not seem to be fulfilled.

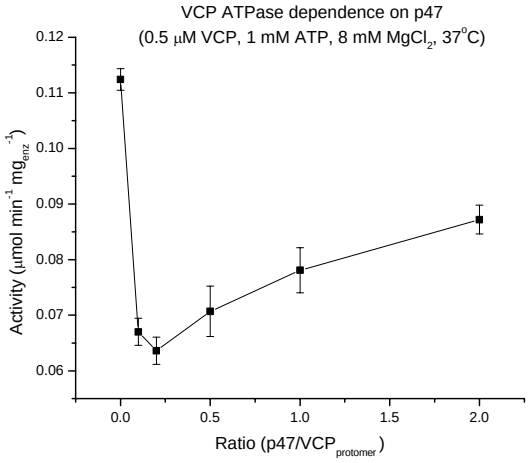

Figure 3.12: ATPase activity of VCP with different amounts of p47.

3.6 VCP mutant K524A

Without the lysine residue involved in ATP binding in the D2 domain one would expect considerably lower hydrolytic activity, and as seen in figure 3.13, this is very much the case. The phosphate release is only about 5 % compared to the wildtype, which also indicates that the wildtype D2 domain contains the dominating hydrolytic site of the ATPase. However, being a binding mutant and not a hydrolysis mutant, the lower rate of ATP hydrolysis due to decreased ATP binding should be possible to overcome by increased ATP concentration. The experiments showed no such indication.

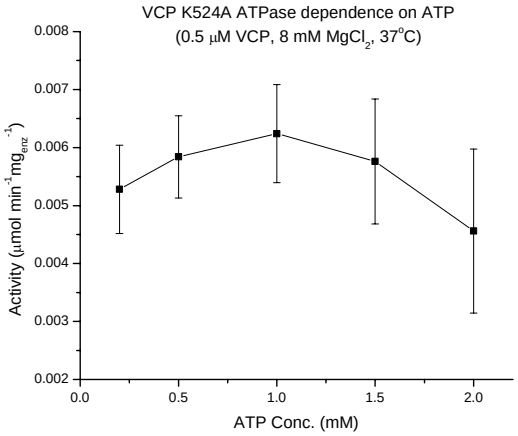

Figure 3.13: ATPase activity of VCP-K524A at different amounts of ATP.

3.7 Binding assays with VCP

An ITC-experiment where ADP was added into a solution of wildtype VCP at 15 degrees gave a relatively good titration curve (figure 3.14). A non-linear regression procedure of the parameters in the Wiseman equation (see section 2.5) gave a binding stochiometry close to one per VCP protomer, indicating that only one of the two nucleotide-binding sites is actually involved in nucleotide binding during the titration. Presumably the D1 binding-domain has bacterial ADP permanently bound. The apparent enthalpy of binding was -5100 ± 300 cal/mol and the dissociation constant 430 ±90 nM.

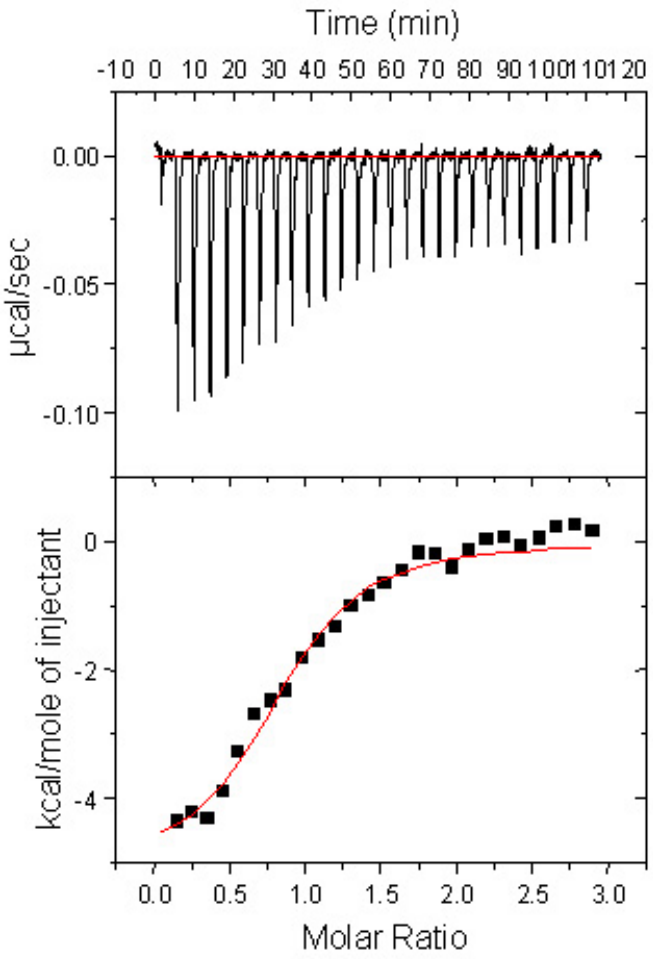

Figure 3.14: Isothermal titration calorimetry of ADP added to VCP. Top: The differential power signal, i.e. the energy it takes to keep constant temperature in the reaction cell. Bottom: The integrated values (Δq_i) per mole of added ADP.

3.8 Structural bioinformatics

The Zn^{2+} species in the central pore that seems to be coordinated by six histidines (His-317) from the D1-domain provided a conspicuous motif (figure 3.15) that was submitted to the Dali database at EMBL for structural homology searches. It would be interesting to see whether this feature has been reported before, and in that case, in what type of proteins. Results from such a search could also, at best, provide important clues to the functionality of VCP. Using the software Pymol, spheres of various sizes were cut out around the Zn ion. They included hexamers of 1 (His-317 only), 2, 6 and 9 residues respectively. Monomers of 9 and 13 residues around his-13 were also created and submitted. However, none of reports from the structural homology searches gave any positive matches, and it may be so that the his/zinc conformation is a new feature whose biological importance is waiting to be discovered.

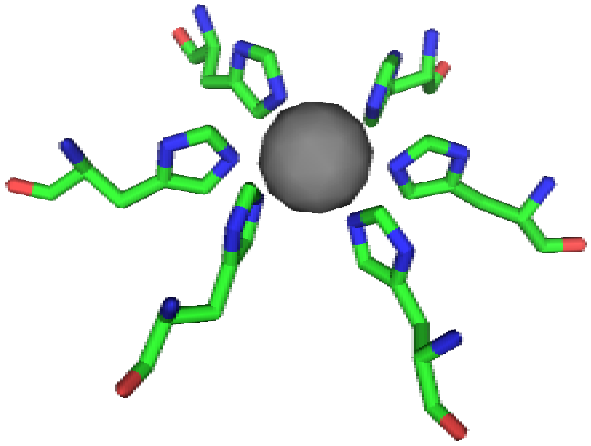

Figure 3.15: The His-317/Zn motif from the D1-part of the central pore.

4. Discussion

The purpose of using Michaelis-Menten theory in this work has not been to find a detailed description for the mechanisms involved in the ATP hydrolysis of VCP or to find individual rate constants or Hill coefficients. The focus has been to establish a method for investigating the biological importance of the enzyme. In order to make comparisons with varied conditions and other experiments, reproducible values of V_{max} and K_M for the enzyme as a whole is of great interest. The plots constructed in this work are relevant and useful, although deviations from ideal fits exist and rough assumptions have been made.

The maximum rate of ATP hydrolysis is estimated to 0.14 $\mu mol*min^{-1}*mg_{enz}^{-1}$, which is equivalent to about 75 molecules of ATP per hexamer of VCP per minute. For protein dislocation, this is a reasonable rate. It corresponds to 12 reaction cycles per minute, or one cycle every 5 seconds (assuming one active site per protomer). If only a few cycles are needed to dislocate a peptide chain from the ER, it could be accomplished on an adequate timescale. However, the physiological rate of hydrolysis is likely to be higher, and the in-vitro conditions constructed for the measurements are of course far from the cellular environment. Only purified VCP, p47 and ubiquitin have been studied. Surely, various other factors and indeed the actual substrate would be needed to find the true maximum hydrolyzing potential of VCP. Finding this maximum rate, however, was not the aim of this work, but rather to establish a method for following the reaction in real time. This provides a means to identify individual components that are important for the biological activity of VCP, and perhaps also their working stochiometry. A number of such components remain to be tested, such as the Npl4-Ufd1 complex (with and without ubiquitin), polyubiquitin and/or poly-ubiquitylated proteins, detergents etc. One way to find substrates of VCP might be to try small centrifuge fractions of cell lysate. Another possible reason for getting an activity lower than physiological could be problems with expression of such a large protein in *E Coli*.

The estimated V_{max} from the continuous flow measurements are lower than earlier studies using endpoint techniques. Coupled assay measurements should be more reliable since one is able to see what actually happens, rather than analyzing the mean of events that took place during a certain time interval. The value of K_M is also lower than in other studies, but the lower value of K_M is reinforced by the relatively low dissociation constant that were calculated from the ITC-experiment (K_M can be seen as an approximation of the dissociation constant of the enzyme-substrate complex).

Three different experiments in this work indicate a functionally and structurally important property of VCP: The D1 nucleotide-binding domain has ADP more or less permanently bound. Its role seems to be to keep VCP in its hexameric state and possibly also to communicate the motions from the ATP hydrolysis that takes place in the D2 domain to other parts of the molecule. VCP looses almost all of its ATPase activity when the lysine involved in nucleotide binding in the D2 domain is mutated, indicating that this domain is responsible for most of the activity of VCP. The ITC indicates only one binding site per protomer (that would be in the D2 domain), and a mutation resulting in nucleotide-binding deficiency in the D1 domain results in failure to form hexamers.

The experiment with VCP + p47 is interesting for two reasons. First, low concentrations of p47 seem to have a negative regulatory effect on VCP, but at higher concentrations - probably as a favorable stochiometry builds up – activity increases. That the activity is still lower than with VCP alone could simply be a lack of the correct substrate. Secondly, earlier published results using endpoint measurements failed to reveal an increase in activity at higher p47/VCP ratios (24), indicating an advantage of the method used in this work.

The big question remains unanswered. What is the actual function of VCP and how is it imparting mechanical force on its substrate? The currently dominating view is that VCP extracts ubiquitylated membrane proteins from the ER and targets them for degradation. Various studies recognize the N-domain as the substrate binding domain, but can enough motion really be transported through two catalytically inactive domains? In EM-reconstructions, the N-domain is only visible in the ADP-AlF_x state, indicating that its conformation is poorly defined or mobile in the other nucleotide states. The possibility remains that there are other binding sites for the substrate, perhaps at the exterior of the hexamer. Another question has been whether a peptide chain could be threaded through the central pore as it is being pulled out of a membrane. It is an appealing idea, but in that case the His317-coordinated zinc would have to be displaced. This seems unlikely however, and the role of the zinc is probably structural stability.

Research on this large hexameric ATPase will no doubt continue and, with the structure at hand, more thorough investigations of the molecular mechanics can be made. Successful results will apply to a large family of ATPases that are involved in many cellular processes.

5. Acknowledgements

I am very thankful to Byron Delabarre, who provided the framework for this project. He provided purified wildtype VCP, strains of mutant VCP and Ni-NTA purified p47. He was responsible for the titration work, helped setting up the light scattering experiments as well as analyzing the data. Also thanks for reviewing the report.

Stephen Kaiser helped me do the mass spectrometry analysis of the VCP-K251A fragments.

Axel Brunger gave me the amazing opportunity to work in his laboratory. Thanks for being my supervisor and providing a motivating atmosphere.

I also want to thank all the members of Brunger lab for making me feel welcome and always giving me a hand when I needed it.

Alwyn Jones helped me get in touch with different labs for my project. Thank you for being my scientific reviewer and a great inspiration to structural biology.

I also thank Jessica Allard and Jonas Söderberg for critical reading and for acting as opponents at my presentation.

6. References

1. Brunger, A.T. Structural insights into the molecular mechanism of calcium-dependent vesicle-membrane fusion. *Curr Opin Struct Biol*. **11**:163-73 (2001).
2. Kondo, H., Rabouille, C., Newman, R., Levine, T.P., Pappin, D., Freemont, P. & Warren, G. p47 is a cofactor for p97-mediated membrane fusion. *Nature* **388**: 75-78 (1997).
3. Latterich, M., Frohlich, K.U. & Schekman, R. Membrane fusion and the cell cycle: Cdc48p participates in the fusion of ER membranes. *Cell* **82**:885-93 (1995).
4. Ye, Y., Meyer, H.H. & Rapoport, T.A. The AAA ATPase CDC48/p97 and its partners transport proteins from the ER into the cytosol. *Nature* **414**:652-6 (2001).
5. Meyer, H.H., Shorter, J.G., Seemann, J., Pappin, D. & Warren, G. A complex of mammalian Ufd1 and Npl4 links the AAA-ATPase, p97, to ubiquitin and nuclear transport pathways. *EMBO J.* **19**:2181-92 (2000).
6. Meyer H.H., Wang, Y. & Warren, G. Direct binding of ubiquitin conjugates by the mammalian p97 adaptor complexes, p47 and Ufd1-Npl4. *EMBO J.* **21**:5645-52 (2002).
7. Neuwald, A.F, Aravind, L., Spouge, J.L & Koonin, E.V. AAA+: A class of chaperone-like ATPases associated with the assembly, operation, and disassembly of protein complexes. *Genome Res*. **9**:27-43 (1999).
8. Lupas, A.N. & Martin, J. AAA proteins. *Curr Opin Struct Biol.* **12**:746-53 (2002).
9. Vale, R.D. AAA Proteins: Lords of the ring. *J Cell Biol.* **150**:F13-9 (2000).
10. Zhang, X., Shaw, A., Bates, P.A., Newman, R.H., Gowen, B., Orlova, E., Gorman, M.A., Kondo, H., Dokurno, P., Lally, L., Leonard, G., Meyer, H., van Heel, M. & Fremont, P.S. Structure of the AAA ATPase p97. *Mol Cell* **6**:1473-84 (2000).

11. Hattendorf, D.A. & Lindquist, S.L. Analysis of the AAA sensor-2 motif in the C-terminal ATPase domain of Hsp104 with a site-specific fluorescent probe of nucleotide binding. *Proc Natl Acad Sci USA* **99**:2732-7 (2002).
12. Hartman, J.J. & Vale, R.D. Microtubule disassembly by ATP-dependent oligomerization of the AAA enzyme katanin. *Science* **286**:782-5 (1999).
13. Whiteheart, S.W., Rossnagel, K., Buhrow, S.A, Brunner, M., Jaenicke, R. & Rothman, J.E. N-ethylmaleimide-sensitive fusion protein: a trimeric ATPase whose hydrolysis of ATP is required for membrane fusion. *J Cell Biol.* **126**:945-54 (1994).
14. Rouiller, I., DeLaBarre, B., May, A.P., Weis, W.I., Brunger, A.T., Milligan, R.A. & Wilson-Kubalek, E.M. Conformational changes of the multifunction p97 AAA ATPase during its ATPase cycle. *Nat Struct Biol.* **9**:950-7 (2002).
15. Webb, M.R. A continuous spectrophotometric assay for inorganic phosphate and for measuring phosphate release kinetics in biological systems. *Proc Natl Acad Sci USA* **89**:4884-7 (1992).
16. 'Light scattering university' course material, Wyatt Technologies, Inc.
17. Johnson Jr, W.C. Protein secondary structure and circular dichroism: A Practical guide. *Proteins* **7**:205-14 (1990).
18. Bernhard Rupp: "Circular dichroism spectroscopy" http://www-structure.llnl.gov/cd/cdtutorial.htm (7 Nov, 2002).
19. Kronig R. de L. & Kramers, H.A. *Atti Congr. Intern. Fisici*, Como 2, 545 (1927).
20. Pierce M.M., Raman, C.S. & Nall, B.T. Isothermal titration calorimetry of protein-protein interactions. *Methods* **19**:213-21 (1999).
21. Jelesarov, I. & Bosshard, H.R. Isothermal titration calorimetry and differential scanning calorimetry as complementary tools to investigate the energetics of biomolecular recognition. *J Mol Recognit.* **12**:3-18 (1999).
22. Indyk, L. & Fischer, H.F. Theoretical aspects of isothermal titration calorimetry. *Methods in enzymology*, vol 295.
23. Pécheur, E.I., Martin, I., Maier, O., Bakowsky, U., Ruysschaert, J.M. & Hoekstra, D. Phospholipid species act as modulators in p97/p47-mediated fusion of golgi membranes. *Biochemistry* **41**:9813-23 (2002).
24. Meyer, H.H., Kondo, H. & Warren, G. The p47 co-factor regulates the ATPase activity of the membrane fusion protein, p97. *FEBS Lett.* **437**:255-257 (1998).